

Joint refinement of a local wave-function model from Compton and Bragg scattering data

J.-M. Gillet, P. J. Becker, and P. Cortona

Laboratoire Structures Propriétés et Modélisation des Solides, CNRS-UMR8580, Ecole Centrale Paris, Grande Voie des Vignes, Chatenay-Malabry Cedex 92295, France

(Received 16 January 2001; published 30 May 2001)

The first joint refinement of a local wave-function model from diffraction and Compton scattering data is reported. The proposed method suits particularly well the case of insulators. Crystalline magnesium oxide, for which both accurate directional Compton profiles and low-order structure factors are available, is chosen as a test case. In particular, it is shown that Compton scattering provides a wealth of additional information to the structure factors in the case of a chemical bond investigation.

DOI: 10.1103/PhysRevB.63.235115

PACS number(s): 78.70.Ck, 71.28.+d, 71.15.-m

I. INTRODUCTION

In the last few decades, structure factors, $F(h,k,l)$, obtained from x-ray or electron diffraction experiments, have been intensively used to study the electron density behavior in crystalline solids. In particular, diffraction data have proved to be very successful at describing the local symmetry around a given nucleus, through the ‘‘multipoles on atoms’’ model.¹ On the other hand, it is also established that the most delocalized part of the electron density, such as the bonding features, are not fully described by this approach.²

Directional Compton profiles (DCP’s) originate from the incoherent inelastic scattering of x rays and therefore provide a quasicontinuous set of data in momentum space. Moreover, it is well recognized that Compton experiments are particularly sensitive to the delocalized features of the electronic wave function.³ The principal disadvantage of Compton data is that they usually suffer from a rather poor statistics originating from the incoherent nature of the scattering process. Since the advent of new x-ray sources such as third-generation synchrotron sources, a dramatic improvement in the quality of Compton data has been achieved. It has thus become possible to treat almost on the same level of accuracy both Bragg and Compton scattering data and possibly make use of their complementarity.⁴ It is the aim of this article to explain a possible joint use of these two different sets of data to refine a model of the electronic wave function.

II. LOCAL IONOCOVALENT MODEL FOR MgO

The structure factors and the Compton profiles are not related in a straightforward manner. On one hand, the structure factors are Fourier transforms of the thermally averaged electron density $\langle\rho(\vec{r})\rangle$:

$$F(\vec{Q}) = \int \langle\rho(\vec{r})\rangle e^{i\vec{Q}\cdot\vec{r}} d\vec{r}. \quad (1)$$

On the other hand, within the impulse approximation,⁵ if $n(\vec{p})$ is the momentum density (quite insensitive to thermal effects), the DCP measured in the direction \vec{u} , is

$$J_{\vec{u}}(q) = \int n(\vec{p}) \delta(\vec{u}\cdot\vec{p} - q) d\vec{p}. \quad (2)$$

One of the challenges is thus to build a unique model to account for both observables since:

$$\rho(\vec{r}) = \sum_i n_i |\varphi_i(\vec{r})|^2, \quad (3a)$$

$$n(\vec{p}) = \sum_i n_i |\tilde{\varphi}_i(\vec{p})|^2, \quad (3b)$$

where $\varphi_i(\vec{r})$ is a natural orbital, of occupation n_i , and $\tilde{\varphi}_i(\vec{p})$ its Fourier transform.

Magnesium oxide crystallizes in a rocksalt structure and is often used as an example of ionic solid. As a consequence, models based on a charge transfer of two electrons from magnesium to the valence orbitals of the oxygen have often been used. This kind of model was partly successful in explaining the results of diffraction experiment,^{6,7} although a charge transfer slightly smaller⁷ gives the closest agreement with experimental data. On the other hand, owing to the diffuseness of the valence functions, the large overlap between neighboring anions (mostly in the [110] direction) is expected to yield a partial redistribution of the charge toward directions with weaker overlap (mostly in the [100] direction). This last hypothesis was supported by previous studies⁸ showing that a linear combination of atomic orbital (LCAO) wave function based on a pure ionic picture does not fully reproduce Compton anisotropies.

A few years ago, we successfully addressed a similar problem for crystalline LiH. It was then demonstrated that a small amount of covalency ($\approx 10\%$) was necessary to reproduce quantitatively the observed anisotropies.⁹ Such an approach is expected to be adequate also in the case of magnesium oxide and is described in the following. At first, deviating from a totally ionic model, one allows the valence electrons to be shared between the oxygen and the six magnesium neighbors, through the following local orbitals:

$$\psi_0(\vec{r}) = N_0 [\phi_0(\kappa_{O_{2s}} \vec{r}) + \lambda_s \chi_0(\kappa_{Mg_{3s}} \vec{r})], \quad (4a)$$

$$\psi_j(\vec{r}) = N_j [\phi_j(\kappa_{O_{2p}} \vec{r}) + \lambda_p \chi_j(\kappa_{Mg_{3s}} \vec{r})] \quad \text{for } j=x,y,z, \quad (4b)$$

where N_0 and N_j are normalization constants. The κ ’s are scaling factors and the λ ’s refer to the amount of covalent character in the bond.

Orbitals of the oxygen anion of $2s$ type and $2p_j$ type are, respectively, $\phi_0(\vec{r})$ and $\phi_j(\vec{r})$. The so-called ‘‘cage functions’’ are symmetry-adapted linear combinations of $3s$ -type atomic functions centered on the six closest magnesium cations:

$$\chi_0(\vec{r}) \propto \sum_{j=x,y,z} \varphi\left(\vec{r} - \frac{a\vec{e}_j}{2}\right) + \varphi\left(\vec{r} + \frac{a\vec{e}_j}{2}\right), \quad (5a)$$

$$\chi_j(\vec{r}) \propto \varphi\left(\vec{r} - \frac{a\vec{e}_j}{2}\right) - \varphi\left(\vec{r} + \frac{a\vec{e}_j}{2}\right), \quad (5b)$$

where a is the lattice parameter of the fcc structure (4.216 Å). Constructing Bloch orbitals from those four local functions, the valence momentum density is then readily obtained:^{9,10}

$$n_{\text{model}}(\vec{p}) = \sum_{\mu\nu} [\sigma^{-1}(\vec{p})]_{\nu\mu} \tilde{\psi}_\mu^*(\vec{p}) \tilde{\psi}_\nu(\vec{p}). \quad (6)$$

σ is the overlap matrix in momentum space:

$$\sigma_{\mu\nu}(\vec{p}) = \sum_{\vec{l}} s_{\mu\nu}(\vec{l}) e^{i\vec{p}\cdot\vec{l}}, \quad (7)$$

where the sum runs over all the lattice vectors and s is the local orbital overlap integral:

$$s_{\mu\nu}(\vec{l}) = \int \psi_\mu^*(\vec{r} - \vec{d}_\mu) \psi_\nu(\vec{r} - \vec{d}_\nu - \vec{l}) d\vec{r}, \quad (8)$$

Directional Compton profiles can then be computed using double integrations of expression (6), as stated in Eq. (2). Such a local approach is also well adapted to a description of diffraction data. Taking advantage of similar Debye-Waller factors for both the oxygen and the magnesium,^{6,7} and assuming the usual separation between the pseudoatoms, one obtains the following expression for the structure factors:

$$F_{\text{model}}(\vec{Q}) = 4[f_{\text{O}_{\text{core}}}(\vec{Q}) + f_{\text{mix}_{\text{valence}}}(\vec{Q})] e^{-B_{\text{O}}(\vec{Q}/4\pi)^2} + 4(-1)^{(h+k+l)} f_{\text{Mg}_{\text{core}}}(\vec{Q}) e^{-B_{\text{Mg}}(\vec{Q}/4\pi)^2}, \quad (9)$$

with

$$f_{\text{mix}_{\text{valence}}}(\vec{Q}) = 2 \sum_{j=0,x,y,z} \int \psi_j(\vec{r}) \psi_j^*(\vec{r}) e^{i\vec{Q}\cdot\vec{r}} d\vec{r}, \quad (10)$$

and where \vec{Q} is a reciprocal lattice vector with the coordinates (h, k, l) .

III. DATA AND CHOICE OF BASIS FUNCTIONS

A set of eight high-resolution DCP's ($\delta q \approx 0.12$ a.u.), corresponding to crystallographic non-equivalent directions ([100], [110], [111], [210], [211], [221], [310], [320]), was collected at the ID15B high-energy (29 keV) inelastic scattering beam line of the European Synchrotron Radiation Facility. For each direction, about 30×10^6 million counts were collected under the Compton peak.¹¹ The low-order experimental structure factors were taken from a paper by Zuo

et al.,⁶ where results of very accurate measurements by a convergent electron beam technique are reported.

In this article, comparisons between theoretical and experimental quantities will be done via difference functions that are known to be more sensitive to the accuracy of the model than the pure data.^{10,6} We will use the structure factor distortion

$$\Delta f(\vec{Q}) = (-1)^{h+k+l} \{F(\vec{Q}) - 4[f_{\text{Mg}^{2+}}(\vec{Q}) - (-1)^{h+k+l} f_{\text{O}}(\vec{Q})]\}/4, \quad (11)$$

where f_{O} refers to the calculated oxygen free atom, and the Compton anisotropies are

$$\delta J_u^-(q) = J_u^-(q) - J_{\text{iso}}(q). \quad (12)$$

The ‘‘isotropic’’ profile, $J_{\text{iso}}(q)$, is not meant to give a real isotropic quantity (as a powder profile would) but is used as a mere reference for comparison. It will be either noted $J_{\text{iso},3}$ when calculated from a weighted average over the three main directions ([100], [110], [111]) or $J_{\text{iso},8}$ when computed using the whole set of eight profiles.

In our case, we need basis functions that are able to simultaneously reproduce the two sets of data. In other words, it is important that, for example, an improvement of the model parameters using Compton profiles alone not only gives good Compton anisotropies but also induces a better agreement between the calculated and the observed structure factors or Δf .

Since Watson's approach¹² to the calculation of doubly charged oxygen, many basis atomic functions were proposed for crystalline magnesium oxyde (see, for example, Refs. 8, 13, 14, and 15 and references therein). Among all the functions available from the literature, we selected the following three basis sets that have in common to be based on a local description of MgO:

(1) For historical reasons, and because they were pointed out by Aikala *et al.*⁸ as the most appropriate to reproduce Compton data, oxygen Hartree-Fock based functions (HF) computed by Pantalides *et al.*¹⁴ were tested.

(2) More recently, Luana and co-workers¹³ proposed an original procedure, the perturbed ion (PI) method, for estimating within the Hartree-Fock scheme, the local wave function of the oxygen embedded in a lattice. According to the authors, this function is expected to give a particularly good estimate of the change in kinetic energy upon crystal formation. It is an interesting feature because the kinetic energy is proportional to the second moment of the isotropic Compton profile.

(3) Finally, localized wave functions for the ions in the crystal can be obtained in the framework of the density-functional theory by the scheme proposed by Cortona.¹⁶ In this scheme, the crystal is partitioned in subsystems (ions in the present case) and the wave functions of the latter are determined by solving a system of coupled equations similar to the Kohn and Sham equations. All the interactions between a subsystem and its environment are taken into account by means of terms entering in the effective potential, terms that are determined self-consistently in the calculation.

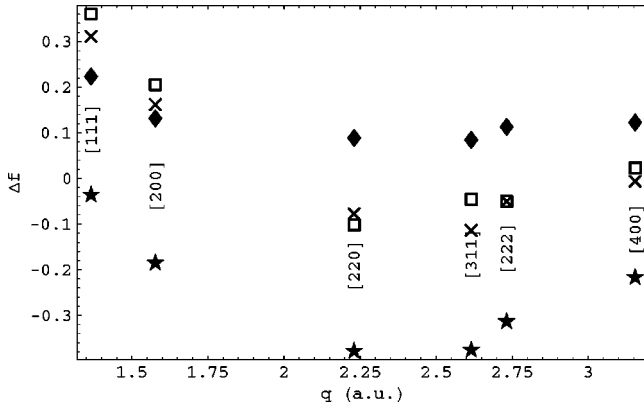


FIG. 1. Comparison of the effect of three different atomic functions on the calculated structure factors after refinement of the local model from three directional Compton profiles. Experiments, squares; HF functions, stars; PI functions, diamond; DFT functions, crosses.

This kind of approach has been successfully applied for studying the standard cohesive properties, the relative stability of the phases and the phase transitions under pressure of ionic solids (for the alkali-earth-metal oxides see Ref. 17).

In order to test for the adequacy of these three sets of basis functions to a joint refinement, a χ^2 fit of the model (χ_J^2) to the three first profiles was first carried out. The only refined parameters were the scaling κ factors for the $2s$ and $2p$ oxygen functions, $\kappa_{O_{2s}}$ and $\kappa_{O_{2p}}$ and the mixing factors, λ_s and λ_p . Figures 1 and 2 summarize the results of a refinement of the local model [Eq. (4)] using the three proposed basis functions from a set of three Compton profiles ([100], [110], [111]). Although the three functions seem to yield correct Compton anisotropies, it appears clearly that the density-functional-theory (DFT)-based functions are most suitable when turning to the structure factor distortion Δf . In addition, these DFT functions also yield a better “isotropic” profile: the mean deviations from experimental values give 0.011 (DFT), 0.019 (PI), and 0.016 (HF) (Fig. 3). In the remainder of this paper, only DFT-based atomic functions will be used.

IV. METHODS FOR THE JOINT REFINEMENTS

Since the local model is expected to describe only the valence electrons, it seemed reasonable to concentrate our attention in the region of reciprocal space where those electrons give the strongest contributions. In that respect, we decided to limit all data within a sphere of 4 a.u. However, it is clear that in such a limited region, for a small cell crystal such as MgO, the structure factors are very sparse. On the other hand, DCP’s data points can be as numerous as the scanning step (or resolution) allow and the number of directions that are probed. We are then facing the following difficulties:

First, the relative weight of structure factors compared to DCP’s can be so weak that no information is gained from a joint refinement using a global χ^2 approach. Second, a refinement procedure using all the Compton directions is

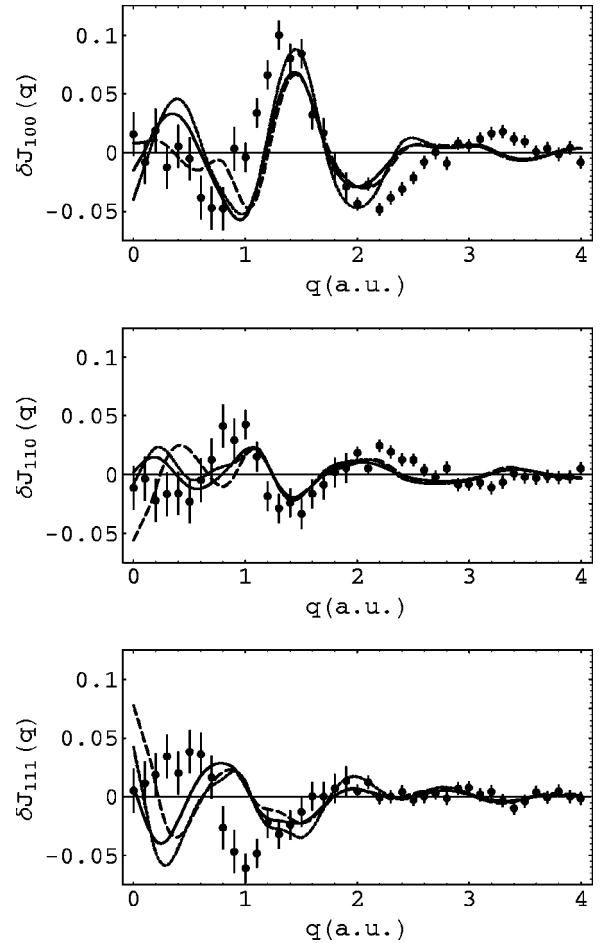


FIG. 2. Comparison of the effect of three different atomic functions on the Compton anisotropies (using $J_{iso,3}$) after refinement of the local model from three directional Compton profiles. Experiments, filled circles with error bars; HF functions, dashed lines; PI functions, dotted lines; DFT functions, solid lines.

bound to be computationally tedious since every iteration requires, for every data point, a double numerical integration of Eq. (6).

To overcome this last technical obstacle, it was then decided to test two different approaches. The first one made use of only three chemically important DCP’s ([100],[110],[111]) and the six structure factors relevant to the above-mentioned sphere in reciprocal space. The second strategy attempted to concentrate as much as possible of the Compton data informations (eight profiles) in a reconstructed electron momentum density (REMD), which was then considered as an observed quantity, with its associated error.

The general problem is then, in both cases, to combine two very different sets of data (in this section, the structure factors, $\{F\}$ and the DCP’s, $\{J\}$) in the refinement of our model, or, equivalently, find the best parameters for the model given two sets of data with undefined relative weights. In words of Bayesian statistics,¹⁸ we are then to maximize, with respect to the parameters $\{\alpha\}$, the probability distribution function (\mathcal{F}_{PDF}) of $\{\alpha\}$, given the sets of data ($\{F\}$ and $\{J\}$) and their associated errors ($\{\sigma_F\}$ and $\{\sigma_J\}$):

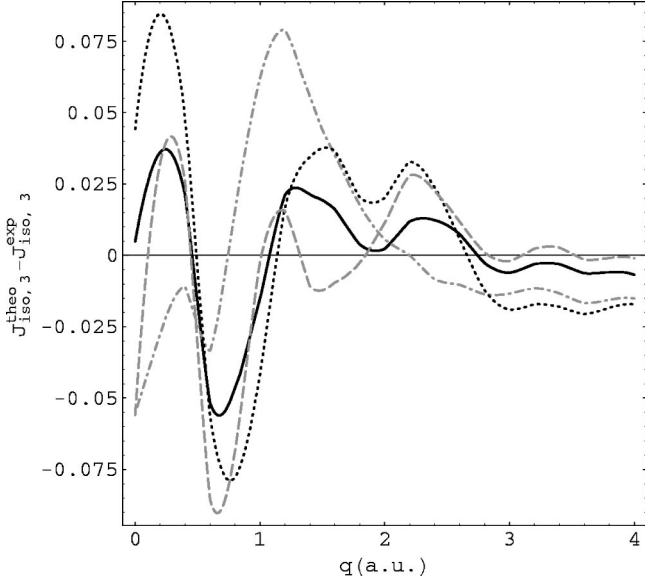


FIG. 3. Difference of $J_{iso,3}^{calc} - J_{iso,3}^{expt}$ for each set of basis functions after refinement of the local model from three directional Compton profiles. HF functions, dashed line; PI functions, dotted line; CRYSTAL92, dotted-dashed line (see Sec. IV A); DFT functions: solid line.

$$\begin{aligned} & \mathcal{F}_{PDF}(\{\alpha\}|\{F\},\{\sigma_F\},\{J\},\{\sigma_J\}) \\ & \propto \mathcal{F}_{PDF}(\{\alpha\}|\{\sigma_F\},\{\sigma_J\}) \\ & \quad \times \int \mathcal{F}_{PDF}(\{F\},\{J\}|\{\alpha\},S_F,\{\sigma_F\},S_J,\{\sigma_J\}) \\ & \quad \times \mathcal{F}_{PDF}(S_F,S_J|\{\alpha\},\{\sigma_F\},\{\sigma_J\}) dS_F dS_J, \end{aligned} \quad (13)$$

where we have assumed an improper knowledge of absolute errors for each set of data by overall scale factors, respectively, S_F and S_J . On the right-hand side of Eq. (13), the forms of the three \mathcal{F}_{PDF} 's had to be postulated. For the first one, a uniform prior form was chosen, assuming that knowing only the errors on the data do not favor any particular values for the parameters. The second \mathcal{F}_{PDF} , likelihood function, is taken as a normal law with uncorrelated data:

$$\begin{aligned} & \mathcal{F}_{PDF}(\{F\},\{J\}|\{\alpha\},S_F,\{\sigma_F\},S_J,\{\sigma_J\}) \\ & \propto \prod_{i,u,j} \exp\left[-\left(\frac{(F^{obs}(\vec{Q}_i) - F^{calc}(\{\alpha\},\vec{Q}_i))^2}{S_F \sigma_F^2(\vec{Q}_i)}\right)\right] \\ & \quad \times \exp\left[-\left(\frac{(J^{obs}(\vec{u},q_j) - J^{calc}(\{\alpha\},\vec{u},q_j))^2}{S_J \sigma_J^2(q_j)}\right)\right]. \end{aligned} \quad (14)$$

This expression is, of course, acceptable only in the limit where the Compton data points are at least separated by one resolution interval. The last \mathcal{F}_{PDF} for the unknown scale factors is assumed to follow Jeffrey's prior form ($\propto 1/S$).¹⁹ It was checked that other prior forms (normalized) did not change significantly the results. Integration over the unknown scale factors, as stated in expression (13), shows that maximizing the \mathcal{F}_{PDF} of $\{\alpha\}$ is equivalent to minimizing a

TABLE I. Numerical values for the parameters of the model obtained from the least squares minimization using the DFT-based functions. All values are dimensionless.

Strategy	$\kappa_{O_{2s}}$	$\kappa_{O_{2p}}$	λ_s	λ_p	Rw_F (R_F) (%)	Rw_J (R_J) (%)
χ_J^2	0.86	1.08	-0.19	0.19	0.6 (0.5)	4.6 (1.7)
$\chi_{F,J}^4$	0.84	1.09	-0.17	0.17	0.2 (0.4)	4.8 (1.9)
$\chi_{REMD,J}^4$	0.90	1.07	-0.14	0.17	0.17 (0.36)	4.5 (1.6) ^a

^aThese values were calculated using the eight Compton profiles.

function, referred thereafter to as $\chi_{F,J}^4$, the product of the χ^2 functions relative to the two sets of data:

$$\begin{aligned} \chi_{F,J}^4 &= [\chi_F^2(\{\alpha\})]^{N_F} \chi_J^2(\{\alpha\})^{N_J} \\ &= \left(\sum_i \frac{[F^{obs}(\vec{Q}_i) - F^{calc}(\{\alpha\},\vec{Q}_i)]^2}{\sigma_F^2(\vec{Q}_i)} \right)^{N_F} \\ & \quad \times \left(\sum_{u,j} \frac{[J^{obs}(\vec{u},q_j) - J^{calc}(\{\alpha\},\vec{u},q_j)]^2}{\sigma_J^2(q_j)} \right)^{N_J}. \end{aligned} \quad (15)$$

where N_F and N_J are, respectively, the numbers of data points from each set. Such a choice will ensure that only the relative variations of the χ^2 functions will be of importance in finding a minimum. The use of $\chi_{F,J}^4$ can then be considered as a reasonable way to counterbalance the weight of the Compton data. It should, however, be noted that assuming total ignorance of the scale factors prevents any direct evaluation of uncertainties on the refined parameters.

A. Joint refinement from directional profiles and structure factors

Refinement of the local wave function, using the DFT-based functions, gives the parameters reported in Table I and yields very good agreement of Δf 's without deteriorating the previous results on the Compton anisotropies. The results of the fit are summarized in Figs. 4 and 5, which should be

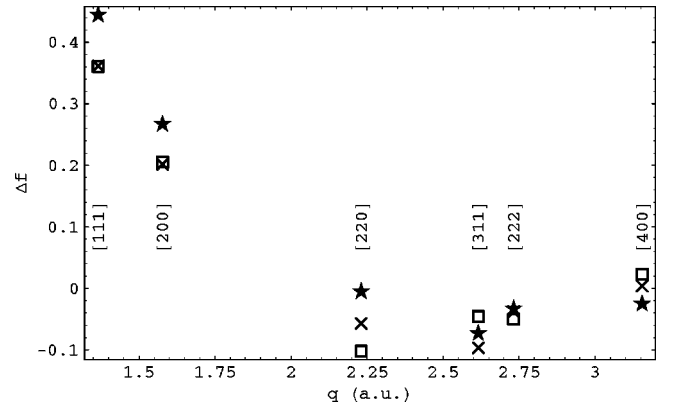


FIG. 4. The Δf function after joint refinement of the local model from a set of six structure factors and three directional Compton profiles (using the $\chi_{F,J}^4$ estimator). Experiments, squares; CRYSTAL92 (with Debye-Waller), stars; DFT functions, crosses.

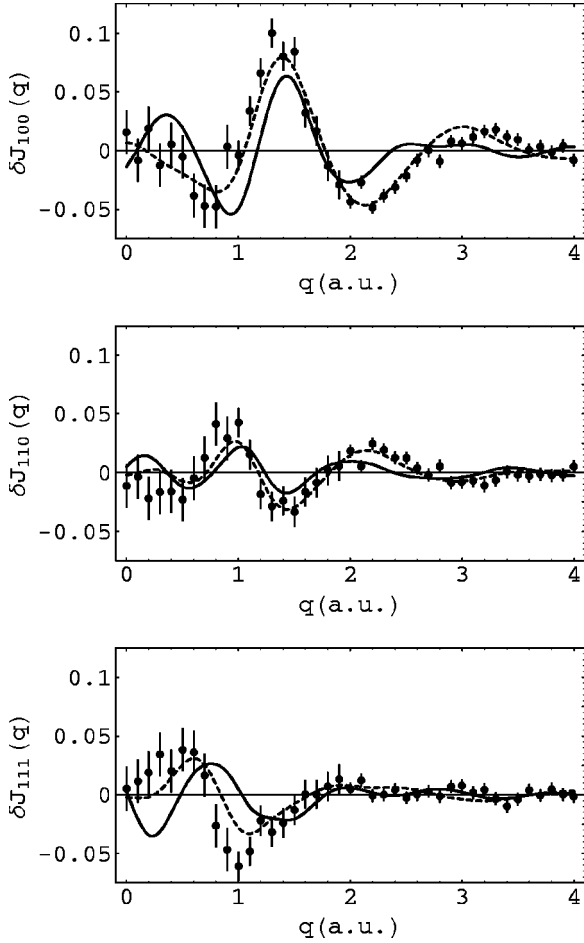


FIG. 5. Compton anisotropies (using $J_{iso,3}$) after joint refinement of the local model from a set of 6 structure factors and 3 directional Compton profiles. Experiments, filled circles with error bars; CRYSTAL92, dashed line; DFT functions, solid line.

compared with Figs. 1 and 2. Given the weakness of the mixing factors, λ 's (line $\chi_{F,J}^4$ in Table I), no κ refinement could be done on the $3s$ -type atomic orbital of magnesium. A global scale adjustment of the structure factors turned out to be of negligible influence (≈ 1.002). A Mulliken population analysis could be carried out for each atom; the charge transfer from the Mg towards O was then estimated to $\Delta q \approx 1.88$, which is in very good agreement with the values previously reported.⁷ Given the crudeness of the local model, it is surprising that the simultaneous agreement with two very different sets of data can be so good. It should, however, be pointed out that no refinement with a simple scaling of atomiclike functions and mixing factors could reproduce the δJ_{111} in a satisfactory manner. *Ab initio* Hartree-Fock calculations, using the CRYSTAL92 code²⁰ with an extended basis set, have been carried out¹¹ and show an almost perfect agreement with experimental anisotropies though, as displayed in Fig. 5, features for direction [111] also tend to be shifted. However, it can be seen in Fig. 3 that CRYSTAL92 results exhibit one of the worst agreements when considering isotropic profiles (mean deviation ≈ 0.017). This point could be interpreted on the basis of electron-electron correlations.²

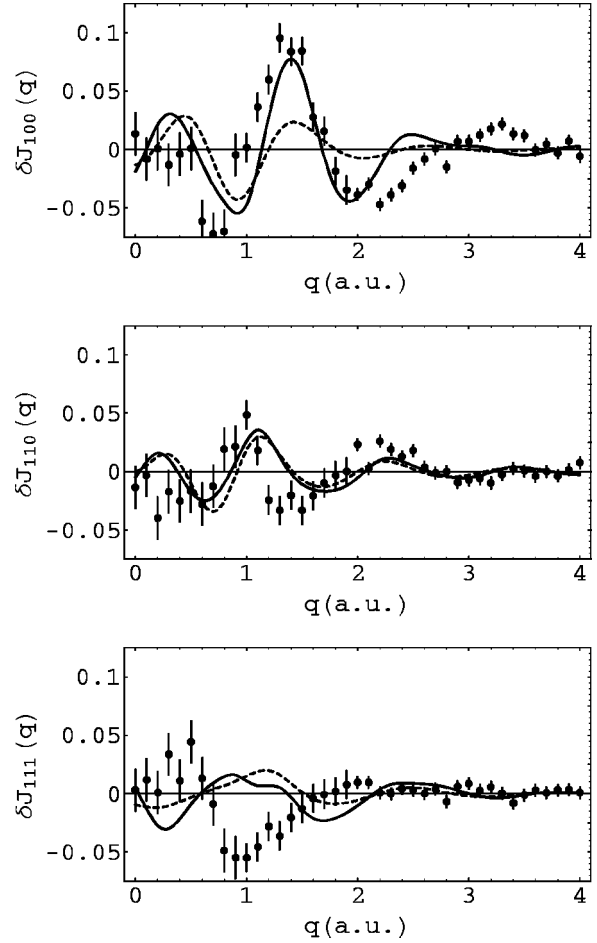


FIG. 6. Compton anisotropies (using $J_{iso,8}$) after joint refinement of the local model from a set of six structure factors and the reconstructed momentum density from the eight DCP's. Experiments, filled circles with error bars; DFT functions, solid line; refinement with $\lambda=0$, dashed line.

B. Joint refinement from reconstructed electron momentum density and structure factors

We already emphasized the reason for using only three DCP's instead of the eight directions that were actually measured; the refinement procedure requires a large number of numerical integrations at every iteration. This is due to the fact that our model is directly related to the momentum density $n(\vec{p})$, but what is actually measured is, for each given direction, a different projection of $n(\vec{p})$. In the general case of systems more complicated than MgO, where more parameters (and orbitals) are needed, it is likely that even a refinement on a limited number of DCP's will be impossible. With that goal in mind, we figured that the best was to use a reconstructed momentum density. Since the pioneer works by Mijnares¹⁰ and Hansen,²¹ many efforts have been put in proposing reconstruction methods, especially during the last five years.^{22–26} As a result, the quality of the reconstructed $n(\vec{p})$ has increased to the point where it could actually be considered as an observed quantity. Thanks to the simplicity of the system, such an approach could be used in the case of LiH using the Hansen reconstruction method.⁹ The analytical

reconstruction method²⁵ has the virtue of providing a simple mathematical expression for $n(\vec{p})$ as well as $\sigma_{n(\vec{p})}$. It is therefore possible to introduce an integral approach to the χ^2 associated with the momentum density and redefine a new estimator for the joint refinement:

$$\begin{aligned} \chi_{F,\text{REMD}}^4 &= \chi_F^2(\{\alpha\}) \chi_{\text{REMD}}^2(\{\alpha\}) \\ &= \sum_i \frac{[F^{\text{obs}}(\vec{Q}_i) - F^{\text{calc}}(\{\alpha\}, \vec{Q}_i)]^2}{\sigma_F^2(\vec{Q}_i)} \\ &\quad \times \int \frac{[n^{\text{rec}}(\vec{p}) - n^{\text{calc}}(\{\alpha\}, \vec{p})]^2}{\sigma_n^2(\vec{p})} d^3p. \quad (16) \end{aligned}$$

Technically, the integration was carried out, in the irreducible part of momentum space, using 300 ‘‘special points.’’²⁷ Minimization of $\chi_{F,\text{REMD}}^4$ has proved to be difficult. In particular, contrarily to the $\chi_{F,J}^4$, all the parameters would yield unphysical results when refined simultaneously. However, when the κ 's were refined separately from the λ 's a minimum could be reached with acceptable values. Results are reported in Table I. Mulliken charge transfer was estimated to 1.83 and Δf values did not show any significant difference with the one obtained in the previous section. Compton anisotropies are plotted in Fig. 6. Although the reference ‘‘isotropic’’ profile were calculated from the eight DCP's,

most anisotropies were of better quality with the noticeable exception of direction [111]. The mean deviation of $J_{\text{iso},8}^{\text{calc}}$ with $J_{\text{iso},8}^{\text{expt}}$ has now improved to 0.009.

V. CONCLUSION

A joint refinement of a simple local orbital model for an ionic crystal from two different sets of data such as x-ray Compton and Bragg scattering was successful. In particular, it was demonstrated that very few parameters, each with straightforward physical interpretation, such as atomic effective screenings and ionocovalency, are able to account for most of the fine experimental features such as Compton anisotropies. It should be pointed out that these last quantities represent, at most, 3% of the total signal on which the refinement is done. A recurrent result, whatever the strategy, is a covalent character of about 3% (estimated with λ^2). The significance of such a small value could be questionable. However, Fig. 6 shows that a refinement, freezing the λ 's to zero, cannot reproduce the Compton anisotropies correctly.

Although more complicated to put into practice, joint refinement from a set of structure factors and reconstructed momentum density is a technique that should be useful for more complicated systems. However, for future developments, a step further would be to use an estimator including correlations due to reconstruction in an expression similar to

$$\chi_{F,\text{REMD}}^4 = \sum_i \frac{[F^{\text{obs}}(\vec{Q}_i) - F^{\text{calc}}(\{\alpha\}, \vec{Q}_i)]^2}{\sigma_F^2(\vec{Q}_i)} \int \frac{[n^{\text{rec}}(\vec{p}) - n^{\text{calc}}(\{\alpha\}, \vec{p})][n^{\text{rec}}(\vec{p}') - n^{\text{calc}}(\{\alpha\}, \vec{p}')]^2}{\sigma_n^2(\vec{p}, \vec{p}')} d^3p d^3p'. \quad (17)$$

Even though MgO is quite an extreme example, this work has shown the possibility to extract simultaneously the basic information present in Bragg and Compton scattering. Essentially structure factors are highly sensitive to relaxation of the shape and symmetry of valence orbitals under crystal forces, but no precise analysis of hopping mechanism of electrons between atoms can be performed from this only experiment. On the contrary, Compton profiles, and more specifically their anisotropies, are highly dependent on the orbital coupling between different atoms.

The major achievement in the present work is the development of a reasonable strategy for refining simultaneously data from both experiments, as discussed in Sec. IV. This

strategy could be easily generalized to the retrieval of informations from measurements of different nature.

ACKNOWLEDGMENTS

The authors would like to thank T. Buslaps and A. Shukla for their support at ESRF and C. Fluteaux, who treated the data and participated in the momentum density reconstruction. D. S. Sivia is greatly acknowledged for sharing with us his insights in Bayesian statistics. J.-B. Kammerer and R. E. Watson are to be thanked for fruitful discussions. J. Jupille is thanked for bringing the MgO charge transfer problem to our attention.

¹P. Coppens, *X-Ray Charge Densities and Chemical Bonding* (Oxford University Press, London, 1997); P. Coppens, *Synchrotron Radiation Crystallography* (Academic, New York, 1992), Sec. 5.3.

²P. Becker, J.-M. Gillet, P. Cortona, and S. Ragot, *Theor. Chem. Acc.* **105**, 284 (2001).

³See, for example, H. Hayashi, N. Udagawa, J.-M. Gillet, W.A. Caliebe, and C.-C. Kao, in *Chemical Application of Synchrotron Radiation*, edited by T.K. Sham (World Scientific, Singapore, in press), and references therein.

⁴Such an attempt to use both Compton and Bragg scattering data was previously done by Schulke and Kramer in tetrahedral co-

- valent crystals. However, only the “forbidden (222)” Bragg reflection was used and no general procedure for simultaneous refinement was proposed [W. Schulke and B. Kramer, *Acta Crystallogr., Sect. A: Cryst. Phys., Diffr., Theor. Gen. Crystallogr.* **35**, 953 (1979)].
- ⁵P. Eisenberger and P.M. Platzman, *Phys. Rev. A* **2**, 415 (1970).
- ⁶J.M. Zuo, M. O’Keefe, P. Rez, and J.C.H. Spence, *Phys. Rev. Lett.* **78**, 4777 (1997).
- ⁷J.-M. Gillet and P. Cortona, *Phys. Rev. B* **60**, 8569 (1999).
- ⁸O. Aikala, T. Paakkari, and S. Manninen, *Acta Crystallogr., Sect. A: Cryst. Phys., Diffr., Theor. Gen. Crystallogr.* **38**, 155 (1982). In this paper, experimental data used for comparison are low-resolution γ Compton profiles.
- ⁹J.-M. Gillet, P.J. Becker, and G. Loupiau, *Acta Crystallogr., Sect. A: Found. Crystallogr.* **51**, 405 (1995).
- ¹⁰*Compton Scattering*, edited by B. Williams (McGraw-Hill, New York, 1977).
- ¹¹C. Fluteaux, Ph.D. thesis, Ecole Centrale Paris, 1999. Valence profiles were evaluated through subtraction of a calculated Hartree-Fock core contribution from the total profiles. No significant deviation from the impulse approximation was observed. The Compton data are available upon request at gillet@spms.ecp.fr.
- ¹²R.E. Watson, *Phys. Rev.* **111**, 1108 (1958).
- ¹³V. Luana, J.M. Recio, and L. Pueyo, *Phys. Rev. B* **42**, 1791 (1990).
- ¹⁴S.T. Pantalides, D.J. Mickish, and A.B. Kunz, *Phys. Rev. B* **10**, 5203 (1974).
- ¹⁵R. Pandey and J.M. Vail, *J. Phys.: Condens. Matter* **1**, 2801 (1989).
- ¹⁶P. Cortona, *Phys. Rev. B* **44**, 8454 (1991); **46**, 2008 (1992).
- ¹⁷P. Cortona and A. Villaforita Monteleone, *J. Phys.: Condens. Matter* **8**, 8983 (1996).
- ¹⁸D. S. Sivia, *Data Analysis, A Bayesian Tutorial* (Oxford University Press, London, 1996), and references therein.
- ¹⁹Sir H. Jeffreys, *Theory of Probability* (Oxford University Press, London, 1998), Chap. III.
- ²⁰R. Dovesi, V.R. Saunders, and C. Roetti (unpublished); M. Causa, R. Dovesi, C. Pisani, and C. Roetti, *Phys. Rev. B* **33**, 1308 (1986); **34**, 2939 (1986); C. Fluteaux, J.-M. Gillet, and P.J. Becker, *Phys. Chem. Solids* **61**, 369 (2000).
- ²¹N.K. Hansen, Report of the Hahn-Meitner-Institut, HMI B342 (1980); N.K. Hansen, P. Pattison, and J.R. Schneider, *Z. Phys. B: Condens. Matter* **66**, 305 (1987).
- ²²R. Papoular (private communication).
- ²³L. Dobrzynski and A. Holas, *Nucl. Instrum. Methods Phys. Res. A* **383**, 589 (1996).
- ²⁴G. Kontrym-Sznajd, M. Samsel, and R.N. West, *Acta Phys. Pol. A* **95**, 591 (1999).
- ²⁵J.-M. Gillet, C. Fluteaux, and P.J. Becker, *Phys. Rev. B* **60**, 2345 (1999).
- ²⁶G. Reiter, J. Mayers, and J. Noreland (unpublished). The method was already mentioned by G. Reiter and R. Silver, *Phys. Rev. Lett.* **54**, 1047 (1985).
- ²⁷Subroutine written by M. Nardelli on the basis of work by J. Hama and M. Watanabe, *J. Phys.: Condens. Matter* **4**, 4583 (1992).